

Nonclassical Bonding in the Novel Structure of Ba_2Bi_3 and Unexpected Site Preference in the Coloring Variant Ba_2BiSb_2

Siméon Ponou and Thomas F. Fässler*

Department Chemie, Technische Universität München, Lichtenbergstr. 4, D-85747 Garching, Germany

Received April 1, 2004

The new phase Ba_2Bi_3 crystallizes in the W_2CoB_2 structure type. Its structure contains rigorously planar anionic layers of $(4.6.4.6)-(4.6^2)_2$ nets with three- and four-bonded Bi, that are separated by Ba atoms. An unexpected site preference is observed in the coloring variant Ba_2BiSb_2 with Sb occupying only the three-bonded sites. The nonclassical bonding in the anionic network can be rationalized from a reformulation of the Zintl concept as $(\text{Ba}^{2+})_2-[\text{Bi}_3]^{3-}(\text{e}^-)$. Bonding distances suggest that the extra electron fills Bi–Bi antibonding states. The densities of states obtained from TB-LMTO-ASA calculations show metallic character for both compounds.

Owing to the significant electronegativity difference between the components, the combination of main group elements with electropositive s-block metals (A and Ae = alkali and alkaline-earth metals, respectively) frequently leads to “polar intermetallic” compounds. When the p-block element, E, is a semimetal, the structure can very often be described using the Zintl–Klemm–Busmann concept¹ whereby all valence electrons are assigned, at least formally, to the electronegative main group elements. The electrons are then localized either in two-center–two-electron (2c–2e) bonds between E atoms or in the form of lone pairs located at these atoms. In the case of metallic p-block elements, the structures are far more diverse and provide more complex aspects of “valence rules” that require an extension of the Zintl concept to accommodate modern bonding concepts such as Wade’s rules, multicenter two-electron bonding, and hypervalency.²

Compounds of a binary phase system (AeE) rich in the electronegative component (E) are excellent candidates to study chemical bonding between E atoms, since the electron count and changes in chemical bonding depend solely on the composition and not on the nature of the atoms. For example, the Sr–Sn system on the tin-rich side shows the transition from a Zintl phase (SrSn) through Sr_3Sn_5 , which

has been described as a formally electron balanced but metallic compound,³ to SrSn_3 and SrSn_4 which still show considerable electron localization and directive bonds, but have predominately metallic bonding characteristics and are both superconducting.⁴

Alkaline-earth antimonides and bismuthides are, with respect to bond characteristics, closely related to binary phases containing tin. On the alkaline-earth rich side, the binaries $\text{Ae}_{11}\text{Pn}_{10}$ (Ae = Ca, Sr, Ba; Pn = Sb, Bi) are Zintl phases featuring isolated Bi^{3-} atoms, Bi_2^{4-} dumbbells besides square planar Bi_4^{4-} units.⁵ However, in the pnictogen rich side the antimonides such as Ae_2Sb_3 (Ae = Sr, Ba)⁶ still have the characteristics of Zintl-phases with molecular Sb_6^{4-} hexamers and semiconducting property, whereas the homologous Bi phase Sr_2Bi_3 is metallic, and its structure cannot be explained by the Zintl concept.⁷ Herein we describe a new compound on the Bi-rich side Ba_2Bi_3 , which can neither be described by the classical Zintl concept, nor with the extended electron counting rules for two-dimensional nets, which have recently been introduced by Hoffmann.⁸ Partial substitution of Bi with Sb shows a strict site preference and gives indications of atomic sites with an enhanced property for electron localization.

Single crystals of Ba_2Bi_3 (**1**) were obtained by reacting stoichiometric amounts of pure elements (with a slight excess of barium).⁹ The powder pattern clearly shows the presence of other unidentified phases in approximately similar amounts. The compound crystallizes in the orthorhombic space group *Immm* and is derived from the W_2CoB_2 structure type,¹⁰ with Bi in Co and B positions. The stoichiometric amount of Ba, Sb, and Bi under similar reaction conditions gave Ba_2BiSb_2 (**2**) in high yield (as revealed by powder diffraction pattern)

* To whom correspondence should be addressed. E-mail: Thomas.faessler@lrz.tum.de.

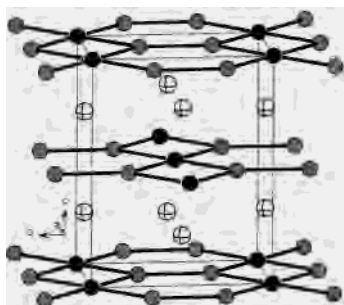
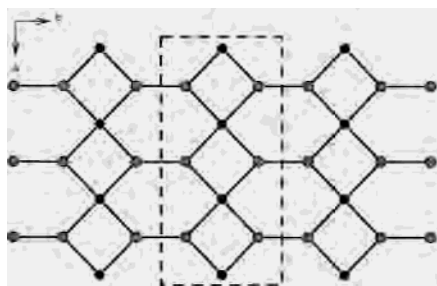
- (1) (a) Zintl, E. *Angew. Chem.* **1939**, 52, 1. (b) Klemm, W. *Proc. Chem. Soc., London* **1958**, 329.
(2) (a) Nesper, R. *Angew. Chem., Int. Ed. Engl.* **1991**, 30, 789. (b) *Chemistry, Structure and Bonding of Zintl Phases and Ions*; Kauzlarich, S. M., Ed.; VCH Publishers: New York, 1996.

- (3) (a) Eckerlin, P.; Meyer, H. J.; Wölfel, E. *Z. Anorg. Allg. Chem.* **1955**, 307, 145. (b) Zürcher, F.; Hoffmann, S.; Fässler, T. F.; Nesper, R. *Z. Anorg. Allg. Chem.* **2001**, 627, 2211.
(4) (a) Fässler, T. F.; Hoffmann, S. *Z. Anorg. Allg. Chem.* **2000**, 626, 106. (b) Hoffmann, S.; Fässler, T. F. *Inorg. Chem.* **2003**, 42, 8748.
(5) (a) Deller, K.; Eisenmann, B. *Z. Naturforsch.* **1976**, 31B, 29. (b) von Schnering, H. G.; Hönlle, W. *Z. Anorg. Allg. Chem.* **1979**, 456, 194. (c) Derrien, G.; Tillard, M.; Manteghetti, A.; Monconduit, L.; Belin, C. *J. Solid State Chem.* **2002**, 164, 169.
(6) (a) Eisenmann, B. *Z. Naturforsch.* **1979**, 34B, 1162. (b) Eisenmann, B.; Jordan, H.; Schaefer, H. *Z. Naturforsch.* **1985**, 40B, 1603.
(7) Merlo, F.; Fornasini, M. L. *Mater. Res. Bull.* **1994**, 29, 149.
(8) (a) Papoian, G. A.; Hoffmann, R. *Angew. Chem., Int. Ed.* **2000**, 39, 2408. (b) Papoian, G.; Hoffmann, R. *J. Am. Chem. Soc.* **2001**, 123, 6600.

Table 1. Data Collection and Refinement Details

chemical formula	Ba ₂ Bi ₃ (1)	Ba ₂ Bi ₁ Sb ₂ (2)
fw	901.62	727.16
space group	<i>Immm</i> (No. 71)	<i>Immm</i> (No. 71)
Z	2	2
unit cell parameters	<i>a</i> = 4.819(2) Å <i>b</i> = 7.989(4) Å <i>c</i> = 9.982(3) Å	<i>a</i> = 4.803(1) Å <i>b</i> = 7.688(2) Å <i>c</i> = 9.900(2) Å
<i>V</i>	384.3(3) Å ³	365.5(2) Å ³
<i>T</i>	293(2) K	293(2) K
<i>D</i> (calcd)	7.792 (g/cm ³)	6.607 (g/cm ³)
μ (Mo K α)	784.4 (cm ⁻¹)	417.7 (cm ⁻¹)
λ (Mo K α)	0.710073 Å	0.710073 Å
R ₁ /wR ₂ (all data) ^{a,b}	0.0898/0.2047	0.0544/0.1384

^a $R_1 = \sum ||F_o| - |F_c|| / \sum |F_o|$; $wR_2 = [\sum [w(F_o^2 - F_c^2)^2] / \sum [w(F_o^2)^2]]^{1/2}$.
^b (**1**) $w = 1/[\sigma^2(F_o^2) + (0.1120 \cdot P)^2 + 14.22P]$, and (**2**) $w = 1/[\sigma^2(F_o^2) + (0.0999 \cdot P)^2]$ where $P = [(F_o^2 + 2F_c^2)/3]$.

**Figure 1.** Projection of the crystal structure of Ba₂BiSb₂: Bi black, Sb (Bi₂ in Ba₂Bi₃) gray, Ba crossed circle.**Figure 2.** Projection of the anionic layer showing interconnected ribbons (outlined by the box): Bi black, Sb/Bi₂ gray.

which adopts the same structure type, and therefore, **2** represents a coloring variant of **1**.

The crystal structures of **1** and **2** were determined by single crystal X-ray diffraction (see Table 1).¹¹ A projection of the structure is shown in Figure 1. In **1** and **2**, the two-dimensional layers of (4.6.4.6)(4.6²)₂ nets of Bi or Bi and Sb, respectively (Figure 2), are separated by Ba atoms. As a result of the ABAB stacking sequence of the 2D layers the Ba atoms (W position in W₂CoB₂) are located above the six-

and four-membered rings of the Bi net in **1** (Sb–Bi net in **2**). Bi1 occupies a four-bonded position with a square planar environment of Bi2 atoms (Sb atoms in **2**). The atoms at a second independent site are three-bonded. These positions are fully occupied with Sb in the case of the ternary phase **2**. Sb labeled in gray in Figure 1 exclusively occupies these positions.

The substitution of Bi by its smaller congener Sb leads to a reduction of the cell volume by approximately 5%. Considering the lattice parameters, this shrinking is highly anisotropic: *a*, *b*, and *c* are reduced by 0.3%, 3.8%, and 0.8%, respectively. The anisotropic lattice compression correlates directly to changes in interatomic distances when going from the Bi to the Sb–Bi sublattice. In **1**, the Bi₂–Bi₂ distance of 3.247(6) Å is close to those found in the three-atom-wide Bi ribbon in LaGaBi₂ (3.2366(5) Å),¹² or in the binaries Ae₁₁–Bi₁₀ (Ae = Sr, Ba) (3.152(3)–3.286(4) Å) where the Bi–Bi bonds are considered to be localized. This bond length, however, is still longer than that of elemental bismuth (3.072 Å). The Bi₁–Bi₂ distance is 3.380(2) Å, which is close to those found in Sr₂Bi₃ (3.13–3.39 Å)⁷ or in the Bi₃⁷⁻ trimers in Eu₁₄MnBi₁₁ (3.397 Å).¹³ Consequently, the complete substitution of Bi₂ by Sb leads to a shorter Bi₁–Sb distance as compared to that of Bi₁–Bi₂. However, on one hand the Bi₁–Sb distance (3.322(1) Å) is reduced by only 1.7% and remains longer than some of the above-mentioned Bi–Bi distances. But on the other hand, the Sb–Sb contact in **2** (3.098 Å) is reduced by 4.6%, if compared to the Bi₂–Bi₂ distance in **1**. The Sb–Sb distance in **2** is still longer than those found in other alkaline-earth antimonides such as Ba₂–Sb₃ (2.866–3.005 Å),^{6b} Ba₁₁Sb₁₀ (2.955–3.047 Å), or Ba₃–Na₂Sb₄ (2.907(2) Å).¹⁴ Comparable bond lengths are observed in nonclassical structures of rare-earth antimonides such as in the square grid in YbSb₂ (3.120 Å) or in the Sb₅ ribbons of the ternary compounds La₁₃Ga₈Sb₂₁ (3.093(1)–3.134(2) Å) and Pr₁₂Ga₄Sb₂₃ (3.109(1) Å).¹⁵

Nonclassical bonding has been described in rare-earth pnictides (Pn), mostly antimonides, and rationalized using a reformulation of the Zintl concept to account for the partial bond order by interpreting longer Pn–Pn bonds as one-electron–two-center bonds or half-bonds, to a first approximation. Longer Sb–Sb bond distances (3.0–3.3 Å) and coordination geometry are found as indicators.¹⁶ The one-dimensional ribbon extending along the *a*-direction (Figure 2) is reminiscent of similar ribbons seen in many ternary antimonides and more recently in LaGaBi₂.¹² Sidewise connection of three-atom-wide ribbons has been described in α -ZrSb₂.^{17,8b} Applying the Zintl–Klemm–Bussmann concept for the title compounds leads to the formula (Ba²⁺)₂[Bi₃]⁴⁻

- (9) Reactions were carried out in niobium ampules sealed on both sides. The samples were first heated at 850 °C for 2 h, then slowly cooled (6 °C/h) down to 500 °C, tempered for 48 h, and subsequently cooled to room temperature. The products are silverish with metallic lustre and highly air-sensitive.
- (10) Rieger, W.; Nowotny, H.; Benesovsky, F. *Monatsh. Chem.* **1966**, *97*, 378.
- (11) X-ray diffraction data on a single crystal were collected on a two-circle Stoe IPDS 2 diffractometer at 293 K with monochromated Mo K α radiation. Numerical absorption correction was made using the program X-Shape (STOE program suite). The structures were solved by direct methods and refined with the aid of the SHELXTL V5.1 software package. Strong absorption problems are reflected in the final residuals (see Table 1).

- (12) Morgan, M. G.; Wang, M.; Chan, W. Y.; Mar, A. *Inorg. Chem.* **2003**, *42* (5), 1549.
- (13) Chan, J. Y.; Wang, M. E.; Rehr, A.; Kauzlarich, S. M.; Webb, D. J. *Chem. Mater.* **1997**, *9*, 2131.
- (14) Chi, L.; Corbett, J. D. *J. Solid State Chem.* **2001**, *162*, 327.
- (15) (a) Wang, B. R.; Bodnar, R.; Steinfink, H. *Inorg. Chem.* **1966**, *5*, 1468. (b) Mills, A. M.; Mar, A. *Inorg. Chem.* **2000**, *39*, 4599. (c) Mills, A. M.; Mar, A. *J. Am. Chem. Soc.* **2001**, *123*, 1151.
- (16) (a) Mills, A. M.; Lam, R.; Ferguson, M. J.; Deakin, L.; Mar, A. *Coord. Chem. Rev.* **2002**, *233–234*, 207. (b) Papoian, G.; Hoffmann, R. *J. Solid State Chem.* **1998**, *139*, 8–21.

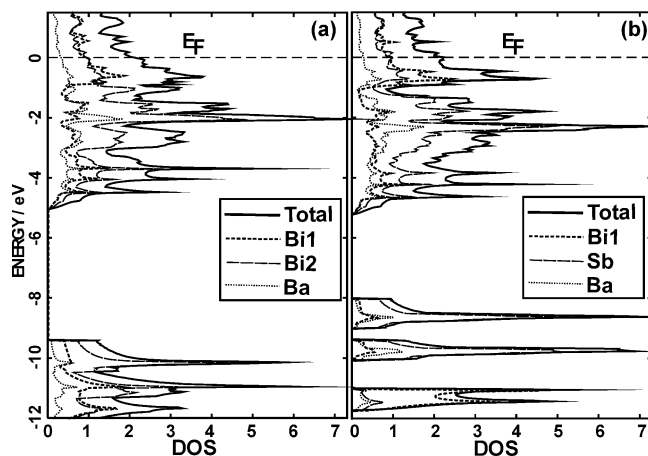


Figure 3. Total and projected density of states (DOS) for (a) Ba_2Bi_3 and (b) Ba_2BiSb_2 ; the Fermi level is taken as point of zero energy.

or $(\text{Ba}^{2+})_2[\text{BiSb}_2]^{4-}$. Using the electron counting procedure proposed by Hoffmann,⁸ isolated infinite three-atom-wide ribbons are stable for an electron count of 20 electrons for three atoms (i.e., $[\text{Bi}_3]^{5-}$). Then, the interconnection of two ribbons such as in the structure of $\alpha\text{-ZrSb}_2$ implies that each atom at the edge lost one electron (if we assumed that the connection is made by classical $2c-2e$ bonds) to give $[-\text{Bi}_3]^{4-}$. In the present compounds, the ribbons are connected at both sides, and the same implementation leads to an electron count of $[-\text{Bi}_3]^{3-}$ or $[-\text{SbBiSb}]^{3-}$ in **2** which results in $(\text{Ba}^{2+})_2[\text{Bi}_3]^{3-}(\text{e}^-)$ or $(\text{Ba}^{2+})_2[\text{Sb}_2\text{Bi}]^{3-}(\text{e}^-)$, respectively. In contrast to $\alpha\text{-ZrSb}_2$ where the interconnection distance is 2.88 Å, the Sb–Sb distance in **2** is 3.098 Å, indicating that the additional electron fills antibonding Sb–Sb states. Since there are considerable Ba states below E_F (see below and Figure 3), we can also assume that there is no full electron transfer from Ba to Bi or Bi/Sb.¹⁸

In **2**, the observed longer Sb–Sb bonds show, however, a higher degree of bond shrinkage as compared to Sb–Bi bonds, which can be understood in terms of a higher degree of electron localization. This fact is also supported by the density of states (DOS) plots obtained from TB-LMTO-ASA calculations.¹⁹ The DOS plots of Ba_2Bi_3 and the partial DOS for Ba, Bi1, and Bi2 calculations are shown in Figure 3a. The orbitals are filled up to the Fermi level E_F , and no band gap is visible around E_F indicating the compound's metallic character. Moreover, the E_F lies at the flank of a local maximum of DOS, suggesting that the compounds are good candidates to exhibit superconductivity.²⁰ The partial DOS projections reveal that the occupied states around E_F are mainly of Bi1 and Bi2 character in accordance with the expected two-dimensional electronic structure. The outstanding differences in the DOS of the substituted Bi_2BiSb_2 (Figure 3b)

are the opening of a deep pseudogap at about 1 eV below the Fermi level and clear separation of the three bands at the bottom of energy scale which are essentially of Bi and Sb s-orbital character. The band at lowest energy has predominantly Bi-s character, probably due to relativistic contraction of the Bi s-orbital. The origin of the pseudogap in Figure 3b traces back to a reduction of Sb states with respect to Bi2 states in **1**. This separation into bonding and antibonding p-orbital states is due to stronger interactions between the neighboring Sb atoms. The contribution of Ba to the DOS is quite significant below the Fermi level, but it drops as we move to E_F . Interestingly, the contribution of Ba at the pseudogap in **2** is reduced and can be interpreted as less interaction between Ba and Sb compared to Ba–Bi interactions in **1**. Although substitution of Bi with Sb leads to a greater degree of electron transfer from Ba to the antibonding states, the states derived from more electronegative Sb lie lower in energy, so that an overall stabilization of the structure may result.

The concept of hypervalency is known to have the capacity to act as an electron sink, which can accept additional electrons to the extent that Pn–Pn bonds are weakened only slightly because of the nonbonding or slightly antibonding character of the states near the Fermi level.^{15a} But due to the expected orbital mixing in the extended anionic layer, the extra electron should normally be delocalized throughout the whole layer. Therefore, the observed strict site preference of Sb in the coloring variant Bi_2BiSb_2 is unexpected. The substitution is of particular interest since both Bi sites in **1** belong to the same polymeric sublattice. This clearly indicates that the site energy and/or bond energy within the anionic layer are different enough to be able to discriminate between two chemically very close elements such as Sb and Bi.

Ba_2Bi_3 and its coloring variant Ba_2BiSb_2 are of great fundamental interest because they are mixed valence compounds of the same atom Bi or of two chemically very close atoms Bi and Sb. Their structures feature rigorously planar anionic layers that can be regarded as a new example of hypervalent geometry. The strict site preference for Sb and the Sb–Sb bond shrinkage gives an indication of atomic sites with an enhanced property for electron localization. This may elucidate some of the aspects of coloring problems in the solid state.²¹ Mixed occupancy of the Bi2 site in **1** by Bi and Sb occurs in the solid solutions $\text{Ba}_2\text{Bi}_{3-x}\text{Sb}_x$ with x varying continuously from 0 to 2 ($x \leq 2$).²²

Acknowledgment. The authors thank the Fonds der Chemischen Industrie for financial support.

Supporting Information Available: Tables of data collection and refinement details, positional and thermal parameters, anisotropic displacement parameters, important distances, and X-ray crystallographic files in CIF format. This material is available free of charge via the Internet at <http://pubs.acs.org>.

IC0495719

(17) (a) Kjekshus, A. *Acta Chem. Scand.* **1972**, *26*, 1633. (b) Garcia, E.; Corbett, J. J. *Solid State Chem.* **1988**, *73*, 440.

(18) Ponou, S.; Fässler, T. F.; Tobías, G.; Canadell, E.; Cho, A.; Sevov, S. C. *Chem. Eur. J.*, in press.

(19) van Schilfgarde, M.; Paxton, T. A.; Jepsen, O.; Andersen, O. K.; Krier, G. In *Programm TB-LMTO*; Max-Planck-Institut für Festkörperforschung: Stuttgart, Germany, 1994.

(20) (a) Fässler, T. F. *Chem. Soc. Rev.* **2003**, *32*, 80–86. (b) Fässler, T. F.; Kronstedt, C. *Angew. Chem.* **1997**, *109*, 2800; *Angew. Chem., Int. Ed. Engl.* **1997**, *36*, 2683.

(21) (a) Miller, G. J. *Eur. J. Inorg. Chem.* **1998**, 523–536. (b) Fässler, T. F.; Kronstedt, C.; Wörle, M. Z. *Anorg. Allg. Chem.* **1999**, *625*, 15.

(22) Ponou, S.; Fässler, T. F. *IXth European Conference on Solid State Chemistry*; Poster abstract P091, University of Stuttgart, October, 2003.